J. Shanghai Jiao Tong Univ. (Sci.), 2017, 22(6): 705-711
https://doi.org/10.1007/s12204-017-1884-7

Responses of the Strata and Supporting System to Dewatering in Deep Excavations

XIAO Xiao (肖　潇), *ZHANG Yangqing* (张扬清), *LI Mingguang** (李明广), *WANG Jianhua* (王建华)
(School of Naval Architecture, Ocean and Civil Engineering, Shanghai Jiao Tong University, Shanghai 200240, China)

Abstract: In order to prevent the inrushing caused by deep excavations, dewatering measure has to be adopted to decrease the confined water level. In this study, the responses of the strata and supporting system to dewatering in deep excavations are investigated through numerical simulations and case studies. Coupled fluid-mechanical analyses are performed by the use of the numerical software, FLAC3D. The responses of the ground settlement, base heave and interior columns to the excavation and dewatering are analyzed. Numerical results indicate that the dewatering measure can effectively reduce the uplift of the subsurface soil in the excavation, and decrease the vertical displacement of the supporting system. In addition, field data of two case histories show the similar responses and confirm the validation of the numerical results. Based on the analyses, dewatering in the confined aquifer is recommended as a construction method for controlling the vertical displacement of the strata and supporting system in deep excavations.
Key words: deep excavations, column, confined water, numerical simulation, dewatering measure
CLC number: TU 473.3　　**Document code:** A

0 Introduction

Because of the shortage of land resources in the city, the height of the buildings had been increasing, which results in deeper basements today than in the past. In order to ensure the safety of these deep excavations, field monitoring was adopted to provide immediate feedback to engineers and the performances of deep excavations had been investigated by analyzing the monitoring data[1-5]. On the basis of the database of 300 deep excavation cases in Shanghai, Wang et al.[6] analyzed the field data of wall displacements and ground settlements. They found that the system stiffness could affect the lateral deformation of the diaphragm wall. Huang et al.[7] focused on the interaction between engineering construction and the geoenvironment and analyzed the natural and anthropogenic causes of the geoenvironmental hazards encountered in the development of underground space. Tan and Li[8] examined the performance of a 26 m deep metro station excavation through a long-term comprehensive instrumentation program. They pointed out that the interior column uplifts and the maximum wall deflections could be described by a linear equation. In addition, numerical method was widely used to predict the effect of deep excavation on underground structures[9-13]. These researches mainly aimed at the effect of deep excavation on the underground structures. However, few paid attention to the problem of dewatering in the confined aquifer.

Due to increase of excavation depth, the thickness of the soil above the confined aquifer is decreased, which will cause water-inrush in the deep excavation. Therefore, the dewatering measure has to be carried out to ensure the safety of underground construction. During the dewatering process, the pore pressure of the soil is decreased and the effective stress of the soil is increased, which will lead to soil compression. Consequently, the deformation of soils and underground structures becomes complex. Thus, it is essential to study the responses of the strata and supporting system to excavation and dewatering. Wu et al.[14] used laboratory tests and numerical simulation to investigate the blocking effect on groundwater seepage under different insertion depths of retaining wall in aquifer. They mainly concerned with seepage. Liu et al.[15] based the finite element method on the Biot consolidation theory and discussed the rationality of the steady state analysis in the dewatering analysis. Tan et al.[16] predicted vertical ground displacements via two types of analyses (transient analysis and steady state analysis) and discussed which one was more accurate. They aimed

Received date: 2016-10-04
Foundation item: the National Natural Science Foundation of China (Nos. 41602283, 41330633 and 41472250)
∗**E-mail:** lmg20066028@sjtu.edu.cn

at the simulation method of dewatering and did not involve excavation couple with dewatering.

In this study, the numerical method is used to simulate the dewatering method during the deep excavation. The results contain the column deformation and soil displacement in the foundation pit. It is expected that with a better understanding of the responses of the strata and supporting system to dewatering in deep excavations, the risks of supporting structures can be avoided due to deep excavation. The results of this study can be helpful for designers and engineers.

1 Numerical Simulation

1.1 Governing Differential Equations

The formulation of coupled deformation-diffusion processes in FLAC3D is done within the framework of the quasi-static Biot theory, and can be applied to problems involving single-phase Darcy flow in a porous medium[17]. According to Darcy's law, the fluid transport is described as

$$\boldsymbol{q}_i = -\boldsymbol{k}_{i,l}\hat{k}(s)[p - \rho_{\mathrm{f}} x_j g_j]_l, \tag{1}$$

where $\boldsymbol{q}_i$ $(i = 1, 2, 3)$ is the specific discharge vector, p is the fluid pore pressure, $\boldsymbol{k}_{i,l}$ $(i = 1, 2, 3;\ l = 1, 2, 3)$ is the tensor of absolute mobility coefficients of the medium, $\hat{k}(s)$ is the relative mobility coefficient which is a function of fluid saturation, ρ_{f} is the fluid density, x_j $(j = 1, 2, 3)$ is the component of coordinate, g_j $(j = 1, 2, 3)$ is the component of the gravity vector, and $[\cdot]_l$ is a partial derivative sign.

1.2 Model Description

The symmetric numerical model is shown in Fig. 1. The distances of the whole foundation model are both 200 m in the x and y directions, and the depth of the model is 80 m in the z direction. The size of the foundation pit is 40 m in the x direction and 40 m in the y direction. The excavation depth of the foundation pit is 22 m. The horizontal constraint is used in two sides of the model, and the horizontal and vertical restraints are adopted in the bottom of the model. The solid element is used to simulate foundation soil, the liner element is used to simulate diaphragm walls, and the beam element is used to simulate struts and piles in the foundation pit. The depths of diaphragm walls and columns are 38 and 50 m respectively, and the thickness of diaphragm walls is 1 m.

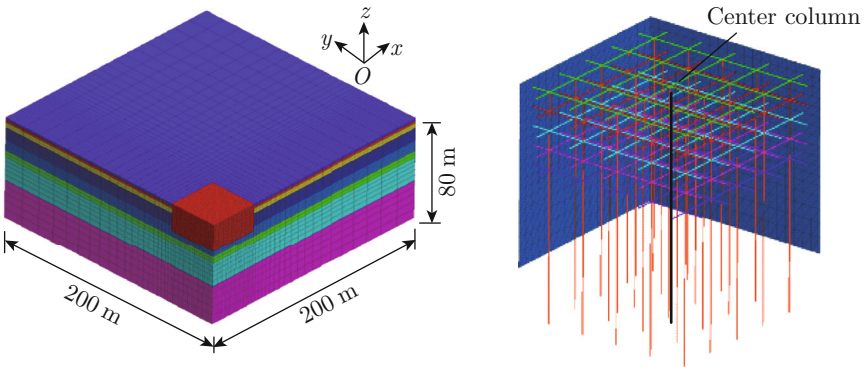

(a) Soil model (b) Structure model

Fig. 1 Mesh for the numerical model

The Mohr Coulomb constitutive model is adopted for the soil. The elastic modulus of the soil is set to $800S_{\mathrm{u}}$[18-19]. The undrained shear strength, S_{u}, can be got from

$$S_{\mathrm{u}} = 20 + 2Z, \tag{2}$$

where Z represents the soil depth. Other parameters of the soil used in the numerical analysis can refer to the foundation design code[20]. The detail parameters of the soil are shown in Table 1, where γ is unit weight, e is void ratio, E is elastic modulus, c is effective cohesion, φ is friction angle, k_{v} is vertical permeability coefficient, and k_{h} is vertical permeability coefficient. The diaphragm walls, piles and struts are set as elastic material; the elastic modulus and Poisson's ratio are set to 30 GPa and 0.2, respectively.

The basic calculation steps of numerical simulation are listed in Table 2. There is no dewatering in the former three steps, until the excavation depth reaches to a certain depth. The anti-uplift formula is

$$\sum h_i \gamma_{\mathrm{s},i} \geqslant F_{\mathrm{s}} \gamma_{\mathrm{w}} H, \tag{3}$$

where h_i is the thickness of each soil layer between the base of the excavation and the top of the confined aquifer, $\gamma_{\mathrm{s},i}$ is the unit weight of each soil layer, γ_{w} is the unit weight of the water, H is the vertical distance between the top of the confined aquifer and the groundwater level of the confined water, and F_{s} is a safety factor.

Table 1 Material properties

Layer	Z/m	γ/(kN·m^{-3})	e	E/MPa	c/kN	φ/(°)	k_v/(m·d^{-1})	k_h/(m·d^{-1})
Backfill	2.0	18.0	0.80	19.6	20	18.0	2.68×10^{-2}	4.32×10^{-2}
Sandy silt	2.0	18.5	0.88	27	4	30.5	2.68×10^{-2}	4.37×10^{-2}
Sandy silt	4.0	18.4	0.88	28	4	31.0	6.48×10^{-2}	1.02×10^{-1}
Silty clay	10.0	16.9	1.36	63	54	11.0	9.16×10^{-5}	1.42×10^{-4}
Clay	9.0	17.9	1.07	105	60	13.5	8.73×10^{-5}	1.02×10^{-4}
Silty clay	4.6	18.2	0.97	150	71	18.0	1.91×10^{-4}	3.06×10^{-4}
Sandy silt	18.5	18.6	0.84	195	3	32.0	2.20	3.55
Clay	29.9	18.0	1.03	284	110	17.0	3.98×10^{-4}	1.71×10^{-3}

As the maximum excavation depth of the foundation pit is 10 m in Step 3, the minimum drawdown of the confined water is 1.252 m with a safety factor of 1.05.

Table 2 Steps of numerical analysis

Step	Computation conditions
1	Excavate to 2 m below the ground surface (BGS)
2	Excavate to 6 m BGS and build the struts
3	Excavate to 10 m BGS and build the struts
4	Dewater the confined aquifer (the accumulative drawdown is 1.25 m)
5	Excavate to 14 m BGS and build the struts
6	Dewater the confined aquifer (the drawdown increment is 6.91 m)
7	Excavate to 18 m BGS and build the struts
8	Dewater the confined aquifer (the drawdown increment is 6.91 m)
9	Excavate to 22 m BGS and build the base plate

1.3 Numerical Results

Dewatering in the confined aquifer can decrease the pore pressure and increase the effective stress, which results in stratum consolidations. Moreover, the movements of the columns and piles might be affected by the dewatering measure due to soil-structure interaction. Therefore, this study only focuses on the responses of the strata and supporting system.

1.3.1 *Vertical Displacement of the Soil*

Figure 2 shows the contours of vertical displacement of the model from the soil cut-plane at $x = 20$ m. It can be seen that the soil inside the pit rebounds and the soil outside the pit settles due to the unloading effect. Figure 3 shows the maximum rebound of the soil inside the foundation pit and the maximum settlement of the soil outside the foundation pit at each step.

In Step 3, the foundation pit is excavated to 10 m BGS, and the maximum vertical displacement of the soil in the foundation pit reaches 32.1 mm. In Step 4,

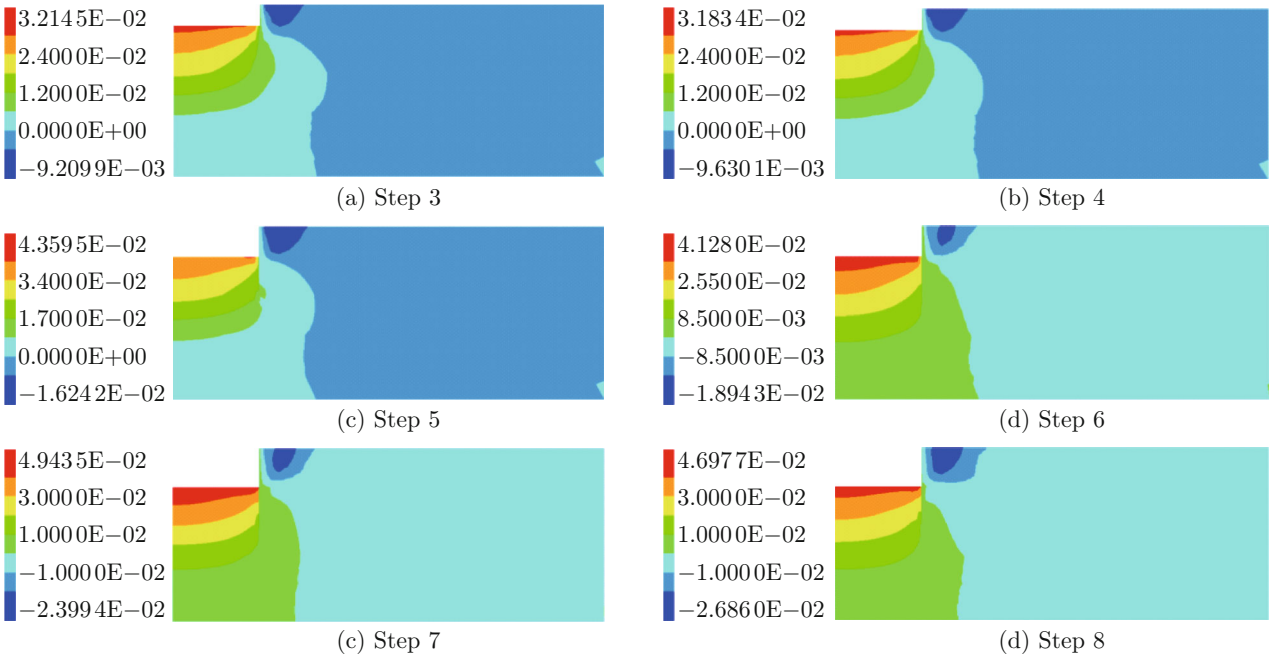

Fig. 2 Contours of vertical displacement of the model from the soil cut-plane (m)

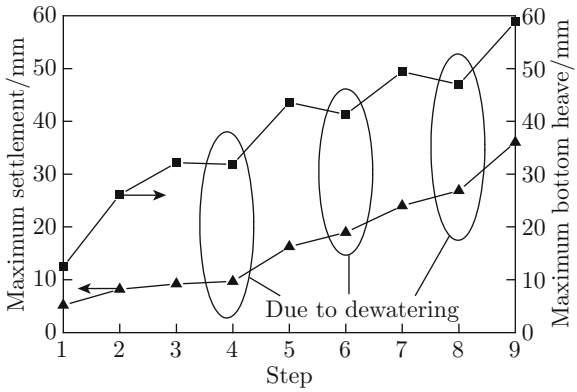

Fig. 3 The maximum rebound of the soil inside the foundation pit and the maximum settlement of the soil outside the foundation pit

the dewatering measure is taken, and the maximum vertical displacement of the soil inside the foundation pit decreases to 31.8 mm. The vertical displacement decreases due to the dewatering measure. Similarly, the maximum vertical displacement reaches 43.6 mm in Step 5 and decreases to 41.3 mm while the second dewatering measure is taken in Step 6. The same responses can be observed from the nephograms of vertical displacement in Steps 7 and 8. At the end of deep excavation, the maximum vertical displacement of the soil inside the foundation pit increases to 58.8 mm. Therefore, it can be tentatively concluded that dewatering in the confined aquifer inside the foundation pit will decrease the rebound of the soil inside the pit. Meanwhile, dewatering may aggravate the settlement of the ground surface soil outside the foundation pit.

1.3.2 *Vertical Displacement of the Column*

Figure 4 illustrates the vertical displacement of center column in association with the construction steps. On the whole, the interior column moves upward continuously with the proceeding of excavation. However, the interior column settles slightly due to dewatering in the confined aquifer. From Step 1 to Step 3, the vertical displacement of the column increases from 4.5 to 17.7 mm. As mentioned above, dewatering has to be carried out prior to further excavation. In Step 4, dewatering is performed with a drawdown of 1.25 m which is the minimum drawdown according to Eq. (3). Results of this step reveal that the dewatering-induced influence on the column is insignificant. With the proceeding of excavation, the drawdown increment increases. Since the excavation depths in Steps 7 and 9 are the same, the required drawdown increments in Steps 6 and 8 are identical (i.e., 6.91 m). It can be seen that the vertical displacement of center column decreases from 21.8 to 19.1 mm in Step 6 and from 25.2 to 22.6 mm in Step 8. As expected, dewatering in the confined aquifer has a great effect on the vertical displacement of center column and the effect increases with the drawdown.

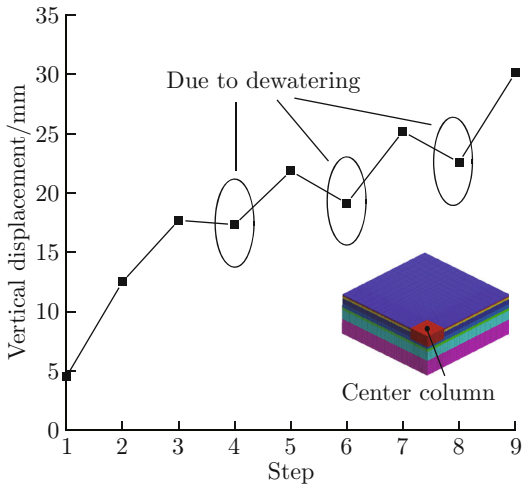

Fig. 4 Curve of vertical displacement at the top of center column

It can be tentatively concluded from the numerical simulation that dewatering in the confined aquifer reduces the upheaval of the soil and center column inside the excavation. In order to verify the numerical results, two cases about deep excavation are selected for analyzing.

2 Case Studies

In this section, the effect of dewatering on the strata and supporting system is analyzed through the field data of two case histories, in which the dewatering measure has been taken. The field data, including the movement of internal column and subsurface soil, are analyzed in association with the excavation depth and drawdown of the confined water.

2.1 Case 1: Shanghai Century Metropolitan Project

Shanghai Century Metropolitan Project is located in Pudong New District, Shanghai. Soil strata at the site consist of nine soil layers with depth to 90 m BGS. The subsoil in the field is mainly soft soils comprising quaternary alluvial and marine deposits. The first confined aquifer is in the seventh layer, and the confined water level is about 3—11 m BGS[21-23].

Figure 5 presents the vertical displacement of subsurface soil movement during the deep excavation, where FC is the measuring point of stratified settlement and the locations of FC1—FC3 are 10, 15 and 20 m BGS, respectively. A1 and B1 are the left and right parts of the foundation pit, respectively. Stages 2—6 of B1 correspond to the excavations of the 2nd—6th layers of the foundation pit, and so on. It can be observed that the vertical displacement of strata settles dramatically prior to Stage 6 of B1. The phenomenon of subsurface soil can be attributed to dewatering.

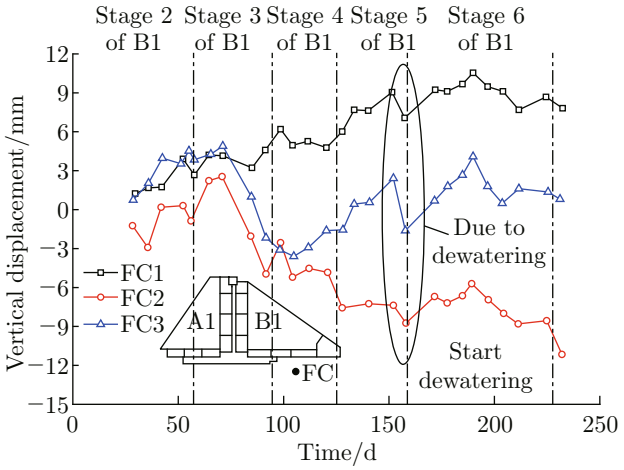

Fig. 5 Vertical displacement of subsurface soil in Shanghai Century Metropolitan Project

Figure 6 depicts the vertical displacement of internal column and diaphragm walls during the deep excavation. It can be seen that the column heaves continuously with the proceeding of excavation. However, the displacement decreases prior to Stage 6 of B1. The maximum vertical displacement of the column reaches 6.8 mm in Stage 5, but it decreases to 2 mm after the dewatering measure is taken. The change of wall displacement is similar to that of the internal column. The vertical displacement of diaphragm walls increases with the increase of the excavation depth until the dewatering measure starts. It is evident that the dewatering measure can effectively reduce the uplift displacement of the column and diaphragm walls during the deep excavation.

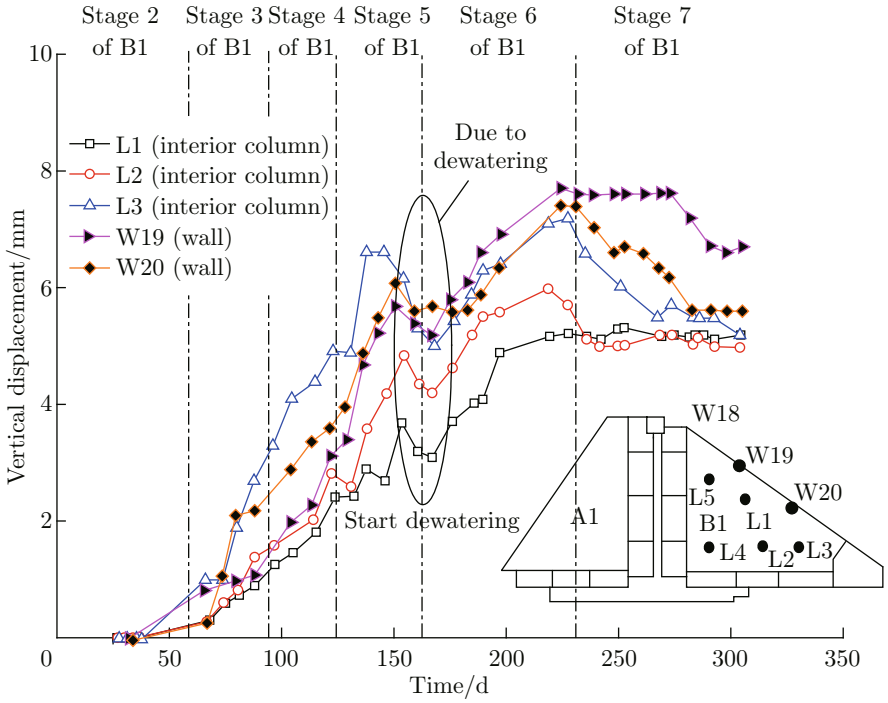

Fig. 6 Vertical displacement of internal column and diaphragm walls

2.2 Case 2: Shanghai Tower

The Shanghai Tower is a megatall skyscraper in Pudong New District, Shanghai. The investigated foundation pit is 17.85—25.89 m deep, with an area of 30 000 m^2. The feature of subsurface conditions is a thick layer of compressible clayey soils in the upper 28 m BGS. The long-term groundwater table level is observed at 0.5—1.2 m BGS. Confined water is encountered at 28 m BGS, and the confined pressure head is 18.2 m. The detail information about the project refers to Ref. [24].

Figure 7 shows the vertical displacement of subsurface soil and the confined water level, where the locations of FC2—FC4 are at 5, 10 and 15 m BGS, respectively. The vertical displacement of the soil outside the foundation pit decreases obviously on the 50th day, and the confined water level changes suddenly. On the 200th day, the confined water level changes again and causes the subsurface soil settlement.

Figure 8 presents the vertical displacement of auger-cast-in-place (ACIP) piles and the confined water level. The data are selected from Stage 8. The confined water level drops rapidly after the 5th day in this stage, and leads to the ACIP pile decline. So, it can be found that dewatering affects the movement of ACIP piles. This phenomenon is similar to that of Case 1. It is consistent with the results obtained in numerical simulation.

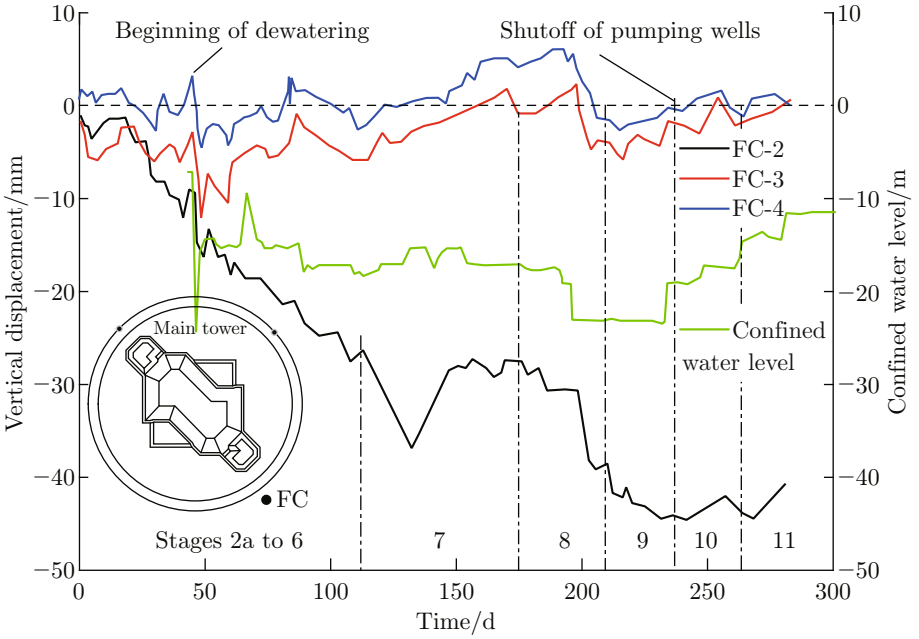

Fig. 7 The vertical displacement of subsurface soil and the confined water level

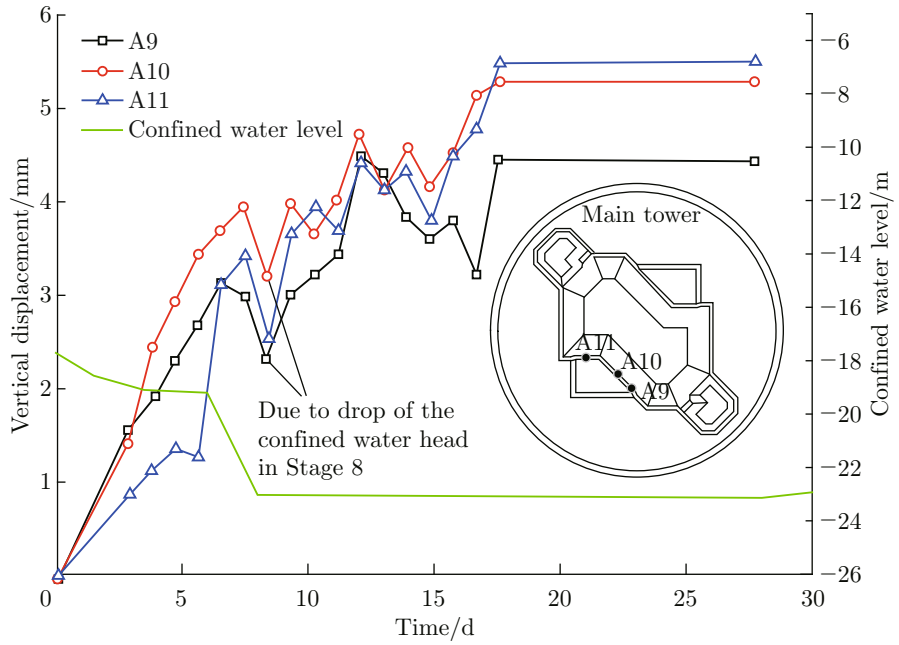

Fig. 8 The vertical displacement of ACIP piles and the confined water level[24]

3 Conclusion

In this study, the effect of dewatering on the subsurface soil and supporting system is analyzed through the numerical simulation in association with two case histories. Based on the above analyses, the following conclusions can be drawn.

Dewatering in the confined aquifer inside the foundation pit decreases the upheaval of the soil inside the pit. However, it may aggravate the settlement of the ground surface soil outside the foundation pit.

Dewatering in the confined aquifer has a great effect on the vertical displacement of interior column and the effect increases with the drawdown of the confined water.

During the deep excavation, the dewatering measure has to be taken to prevent the inrushing caused by deep excavation. This measure can be used to control the deformation of the strata inside the pit and the displacement of internal column.

References

[1] OU C Y, HSIEH P G, CHIOU D C. Characteristics of ground surface settlement during excavation [J]. *Canadian Geotechnical Journal*, 1993, **30**(5): 758-767.

[2] NG C W W. Observed performance of multipropped excavation in stiff clay [J]. *Journal of Geotechnical and Geoenvironmental Engineering*, 1998, **124**(9): 889-905.

[3] MOORMANN C. Analysis of wall and ground movements due to deep excavations in soft soil based on a new worldwide database [J]. *Soils and Foundations*, 2004, **44**(1): 87-98.

[4] WANG Z W, NG C W, LIU G B. Characteristics of wall deflections and ground surface settlements in Shanghai [J]. *Canadian Geotechnical Journal*, 2005, **42**(42): 1243-1254.

[5] O'ROURKE T D, MCGINN A J. Lessons learned for ground movements and soil stabilization from the Boston Central Artery [J]. *Journal of Geotechnical and Geoenvironmental Engineering*, 2006, **132**(8): 966-989.

[6] WANG J H, XU Z H, WANG W D. Wall and ground movements due to deep excavations in Shanghai soft soils [J]. *Journal of Geotechnical and Geoenvironmental Engineering*, 2010, **136**(7): 985-994.

[7] HUANG Y, BAO Y J, WANG Y H. Analysis of geoenvironmental hazards in urban underground space development in Shanghai [J]. *Natural Hazards*, 2015, **75**(3): 2067-2079.

[8] TAN Y, LI M W. Measured performance of a 26 m deep top-down excavation in downtown Shanghai [J]. *Canadian Geotechnical Journal*, 2011, **48**(5): 704-719.

[9] SHARMA J S, HEFNY A M, ZHAO J, et al. Effect of large excavation on deformation of adjacent MRT tunnels [J]. *Tunnelling and Underground Space Technology*, 2001, **16**(2): 93-98.

[10] ZDRAVKOVIC L, POTTS D M, ST JOHN H D. Modelling of a 3D excavation in finite element analysis [J]. *Géotechnique*, 2005, **55**(7): 497-513.

[11] KUNG G T C, OU C Y, JUANG C H. Modeling small-strain behavior of Taipei clays for finite element analysis of braced excavations [J]. *Computers and Geotechnics*, 2009, **36**(1/2): 304-319.

[12] HONG Y, NG C W W. Base stability of multi-propped excavations in soft clay subjected to hydraulic uplift [J]. *Canadian Geotechnical Journal*, 2013, **50**(2): 153-164(12).

[13] HUANG Y, YANG Y, LI J L. Numerical simulation of artificial groundwater recharge for controlling land subsidence [J]. *KSCE Journal of Civil Engineering*, 2015, **19**(2): 418-426.

[14] WU Y X, SHEN S L, YIN Z Y, et al. Characteristics of groundwater seepage with cut-off wall in gravel aquifer I: Field observations [J]. *Canadian Geotechnical Journal*, 2015, **52**(10): 108-116.

[15] LIU J, CHEN J J, WANG J H. Fluid-structure coupling analysis of dewatering and excavation in 500 kV Shanghai Expo underground substation [J]. *Journal of Shanghai Jiao Tong University*, 2010, **44**(6): 721-725 (in Chinese)

[16] TAN Y P, CHEN J J, WANG J H. Practical investigation into two types of analyses in predicting ground displacements due to dewatering and excavation [J]. *Journal of Aerospace Engineering*, 2014, **28**(6): A4014001.

[17] Itasca Consulting Group Inc. FLAC3D V.5.0: Fast Lagrangian analysis of continua in 3 dimensions [Z]. Minnesota: Itasca Consulting Group Inc, 2016.

[18] DONG Y P, BURD H J, HOULSBY G T. Finite-element analysis of a deep excavation case history [J]. *Géotechnique*, 2015, **66**(1): 1-15.

[19] OU C Y, HSIEH P G, LIN Y L. A parametric study of wall deflections in deep excavations with the installation of cross walls [J]. *Computers and Geotechnics*, 2013, **50**(5): 55-65.

[20] Shanghai Municipal Commission of City Development and Transport. Foundation design code: DGJ08-11-2010 [S]. Shanghai: Shanghai Xian Dai Architectural Design (Group) Co., Ltd., 2010.

[21] CHEN J J, WANG J H, XIANG G W, et al. Numerical study on the movement of existing tunnel due to deep excavation in Shanghai [J]. *Geotechnical Engineering Journal of the SEAGS and AGSSEA*, 2011, **42**(3): 30-40.

[22] SHI J W, LIU G B, HUANG P, et al. Interaction between a large-scale triangular excavation and adjacent structures in Shanghai soft clay [J]. *Tunnelling and Underground Space Technology*, 2015, **50**: 282-295.

[23] WANG W, DOU J Z, CHEN J J, et al. Numerical analysis of the soil compaction degree under multi-location tamping [J]. *Journal of Shanghai Jiao Tong University* (*Science*), 2017, **22**(4): 417-433.

[24] TAN Y, WANG D L. Characteristics of a large-scale deep foundation pit excavated by the central-island technique in Shanghai soft clay. I: Bottom-up construction of the central cylindrical shaft [J]. *Journal of Geotechnical and Geoenvironmental Engineering*, 2013, **139**(11): 1875-1893.